Oceanographic conditions in the Gulf of Mexico in July 2010, during the Deepwater Horizon oil spill

GREEN = RYAN GREY = LIBBY YELLOW = MICHELLE BLUE = JOHN LAMKIN

RED = CHRIS

Potential Co-Authors:

R. Smith, E. Johns, R. Lumpkin: hydrographic data, figures, tables, and analysis

G. Goni and J. Trinanes: satellite data, figures, and analysis

C. Kelble: flow-through data / surface water property tables and spatial analysis

S. Cummings: assessment of CDOM optical sensors as an oil indicator

A. M. Wood: LSU oil data assessment (analysis, comparison to other DWH work, incorporation of LSU results, and other efforts to find oil, O2..- with Lamkin and Privoznik)

J. Lamkin and S. Privoznik – net tow / search for tar ball procedure

Abstract

The upper ocean dynamics in the Gulf of Mexico (GOM) are dominated by mesoscale features that include the Loop Current (LC), the Loop Current Rings (LCRs) that it periodically sheds, and adjacent cyclonic eddies. ~~Following the April 20, 2010 explosion at the Deepwater Horizon (DWH) oil drilling site, ~~D~~d~~uring May and June 2010 when~~at a time when~~ oil was still flowing freely from the failed riser of the Deepwater Horizon~~WH~~ drilling rig, a result of its explosion on April 20, 2011, surface drifter trajectories, satellite observations, and numerical simulations in the GOM indicated a potential for direct connectivity between the northern Gulf and the Florida Straits via the LC system. Such a pathway ~~had the potential to~~would potentially entrain particles, including contaminants present in the northern GOM related to the DWH oil spill, and carry them directly towards distant coastal ecosystems in south Florida and northern Cuba, and into the Gulf Stream.

In an effort to assess the connectivity between the spill site and these downstream regions, to determine the potential for of DWH contaminant spreading via the dominant circulation features present in the Gulf, and to evaluate the potential impacts of such contaminants on economically important GOM pelagic fisheries, an interdisciplinary shipboard survey was conducted across the eastern Gulf in July 2010. Analysis of the resulting *in situ* measurements of water column velocity and hydrographic ~~properties confirmed~~properties confirmed concurrent remotely-sensed surface observations, which indicated that during July 2010 a direct transport mechanism was no longer in place, and that a large anticyclonic LCR (named Eddy Franklin) had become separated from the main LC by a cyclonic eddy. As a result, only indirect pathways through the region remained. Additionally, with the exception of 4 hydrographic stations occupied within 84 km of the wellhead as part of this survey, no evidence of oil was found within the study domain (from the surface to a depth of 2000 m), suggesting that any oil entrained by circulation features in the months prior to the cruise had either weathered, been dispersed to undetectable levels, or was only present in unsurveyed areas.

1. Introduction

Following the explosion and sinking of the Deepwater Horizon (DWH) MC252 drilling platform on April 20, 2010, the Gulf of Mexico (GOM) was subjected to the largest anthropogenic crude oil spill ever recorded in the western hemisphere (Adcroft et al. 2010; Liu et al. 2011). Oil flowed continuously from the damaged wellhead for 87 days until it was capped on July 15, 2010. This oil spill event differed from most previous spills in that it occurred in deep water (~1500 m) in the open ocean, in a region affected by strong surface and subsurface currents. Indeed, Kaiser and Pulsipher (2007) state that, as of 2000, only 11% of the total volume of oil spills had occurred offshore in the open ocean, whereas 50% was spilled from oil tankers near the coast. This environment was suitable for the potential transport of oil and dispersants to remote areas beyond the Mississippi Canyon where the spill occurred. Therefore, concerns quickly mounted regarding the extent to which oil could potentially spread to the rest of the GOM in the surface and subsurface (Kaiser and Pulsipher 2007; Adcroft et al. 2010; Liu et al. 2011) aided by the Loop Current (LC), Loop Current Rings (LCR), and adjacent cyclonic eddies, the predominant circulation features of the GOM.

Throughout the spill, the emergency response and scientific communities primarily utilized blended remotely-sensed environmental observations with limited *in situ* measurements to monitor the GOM conditions beyond the immediate spill site. The surface circulation was monitored using a suite of satellite observations, including satellite altimeters (for sea surface height), Synthetic Aperture Radar (SAR, for sea surface roughness and relative velocity), ~~and~~ sea surface temperature (SST) and ocean color imagery (both utilized to identify frontal boundaries and the spatial extent of GOM circulation features at the sea surface). These observations were validated by a limited number of satellite-tracked surface drifters deployed in support of the monitoring efforts. All observations were analyzed in order to monitor the upper ocean dynamics and to identify the pathways by which oil and dispersants could potentially translate from the spill site into other regions of the GOM and beyond. Additionally, several numerical models, such as the HYbrid Coordinate Ocean Model (HYCOM), the U.S. Navy Intra-Americas Sea Nowcast/Forecast System (IASNFS), and the National Oceanic and Atmospheric

Administration Real-Time Ocean Forecast System (NOAA RTOFS) were employed to simulate the GOM circulation at the surface and subsurface.

At the time of the DWH platform explosion, circulation in the GOM was dominated by a "mature" LC (the LC had not shed a ring since July 2009), which extended well into the northern Gulf to approximately 28°N (Figures 1a and 1b). In such a configuration, the possibility for entrainment and delivery of contaminants from northern Gulf waters, including discharge from the Mississippi River, to downstream regions such as the Florida Straits via the LC is historically well documented, and can occur in as little as two to three weeks (Ortner *et al.*, 1995; Hu *et al.*, 2005). To a great extent, this transport mode bypasses the west coast ~~of Florida~~of Florida due to the "forbidden zone" effect associated with the broad west Florida shelf (Yang et al. 1999; Sturges et al. 2001) delivering particles directly to the Florida Straits and adjacent coastal ecosystems such as the Florida Keys. Shown in Figure 2, for the period July 1999-June 2010, a total of 45 drifters traveled within three degrees latitude and longitude of the spill site. Their subsequent trajectories indicate a strong tendency to eventually enter the LC, the Florida Straits, and ultimately the Atlantic basin. Of these drifters, a total of 38 lived long enough to enter the LC, with 20 of these subsequently passing between South Florida and the Bahamas. In addition to early observations, this entrainment scenario was also suggested by early model results utilized to evaluate the potential spreading of surface oil from the spill (Liu *et al.*, 2011; Srinivasan *et al.*, 2010).

In May 2010, the LC began to shed a large LCR (named Eddy Franklin, EF), which at times over the following month appeared to remain in a state of partial attachment with the LC, complicating downstream connectivity and surface oil spreading analyses. Additionally, due to the ~~sparcity~~scarcity of *in situ* surface and subsurface observations in the LC and EF, the extent to which a direct and/or indirect pathway existed between the oil spill site and the rest of the GOM during this period (May and June 2010) was based largely upon analysis of satellite observations, numerical model simulations, and Lagrangian surface drifter trajectories (Figures 1 and 2).

To address the lack of *in situ* observations, the NOAA Atlantic Oceanographic and Meteorological Laboratory (AOML) and National Marine Fisheries Service (NMFS) Southeast Fisheries Science Center (SEFSC), utilizing the NOAA Ship *Nancy Foster*, jointly collected interdisciplinary oceanographic observations across the eastern GOM between June 30 and July 18, 2010 (Figure 3). The primary objectives of this shipboard survey were to assess the physical connectivity between the complex eddy field formed by the LC, EF, and other associated cyclonic frontal eddies which developed over May and June, to document and sample any petroleum contaminants observed in the region, and to determine the potential impacts of any petroleum contaminants on pelagic fish larvae recently spawned in the eastern GOM. This survey was one of only two research cruises conducted during the summer months of 2010 focused on evaluating the potential connections between northern Gulf waters and the southeast coast of Florida, the northern coast of Cuba, and the Straits of Florida.

This paper examines the ambient oceanographic conditions in the GOM between May and August 2010, with an emphasis on velocity and hydrographic data obtained during this July research cruise. The main objective of the paper is to report the degree of connectivity between the immediate oil spill site, the southeastern GOM, and the Florida Straits. A background discussion of the major circulation features and water masses of the GOM is given in Section 2. Observational methods, including a description of measurements and samples collected during the July survey, are described in Section 3. Satellite-derived and Lagrangian drifter data are also described in this section. In section 4 the results of the July 2010 cruise are described, and the hydrographic and satellite data are evaluated to assess the connectivity between the various ocean features. Results of the analysis, described in Section 4, are linked to other environmental and ecosystem observations that could provide information on the presence of oil at the surface and/or subsurface. Section 5 provides a discussion regarding how the synoptic GOM circulation observed during July 2010 compares with what was previously known about the GOM, and how it ultimately influenced the pathways of the dispersal of oil from the DWH spill site.

2. Background - Gulf of Mexico circulation features and water masses

The general circulation and water masses of the GOM, including the LC, LCRs, and the cyclonic eddy field, have been the subject of much study over the past four decades, with the observational study methods systematically progressing over time from shipboard hydrographic observations, satellite SST, satellite-tracked surface drifters, current meters, aircraft observations, satellite ocean color, satellite altimetry, and inverse methods, to sophisticated numerical models. The development of improved instrumental and modeling techniques~~, and the literature that has been published on the results,~~ have led to a much greater understanding of the GOM which has been reflected in several comprehensive and informative review articles (Hofmann and Worley 1986; Oey et al. 2005a; Sturges and Kenyon 2008). The major oceanographic features of the GOM will be briefly reviewed from the literature in the following sub-sections.

A. The Loop Current (LC)

The dominant circulation features of the GOM are the LC, the portion of the Atlantic western boundary current connecting the Caribbean and Yucatan Currents with the Florida Current and the Gulf Stream, and the anticyclonic LCRs that it periodically sheds. Beginning with the early hydrographic studies in the 1960's and 1970's and continuing with the more sophisticated techniques listed above, our knowledge about the LC has accumulated over time.

In one of the pioneering oceanographic studies of the GOM and the LC, Nowlin and McLellan (1967) used a 7-week cruise to describe a synoptic "snapshot" of the entire Gulf. The general circulation patterns that they found (the LC, large LCR, and smaller cyclonic eddies) agree fairly well with what is now known, considering the paucity of data available to them.

Leipper (1970) used a series of eight 2-week cruises to quantify the LC, finding a volume transport of >25 Sv and surface velocities of 50-200 cm/s, and to observe the LCR shedding process in detail for the first time. At this time, there was an impression that the LCR shedding process was a seasonal phenomenon. Soon after this, Cochrane (1972) described the important role of cyclonic eddies in the LCR shedding process, and Nowlin (1972) speculated that local LC dynamics, rather than seasonality, might actually be driving the LCR shedding process.

Behringer et al. (1977), using hydrographic data from 47 cruises to the GOM, described the mean GOM circulation as consisting of the LC growing northward in winter/spring and shedding a LCR in summer, which then drifts west in the fall causing the mean circulation there to tend to form an anticyclonic gyre while the LC shrinks back to the south. They noted, however, that there was considerable variability in any given month.

B. Loop Current Rings (LCRs)

Warm-core LCRs have also been the subject of considerable study. Elliott (1982) used the accumulated hydrographic data set to quantify LCR length scales and translational velocities, and considered their role in the GOM heat and salt balances. He estimated from his salt balance computations that approximately one LCR formed per year, having an average radius of 183 km with a range of 102 to 244 km, and that their average westward translational velocity was 2.1 km/day to 279 degrees. The average transport of LCRs was found to be 29 Sv, in good agreement with previous estimates and with what is known about the transport of the LC from which they originate.

Vukovich and Crissman (1986) looked at LCRs using satellite IR SST imagery and ship-of-opportunity data from 1973-1984. They found that there were three characteristic LCR translation pathways: to the northwestern Gulf, to the middle-western Gulf, and to the southwestern Gulf, but noted that all of the pathways eventually led to the area 25-28^{o}N, 96-93^{o}W. LCR translational speeds were on the order of 1 to 8 km/day~~, with~~, with an average of about 5 km/day, somewhat faster than the translational velocity of 2.1 km/day determined by Elliott (1982) using a more limited data set.

Vukovich (1995) used satellite IR and early satellite ocean color (CZCS) imagery in conjunction with shipboard data to generate a 22-year time series of the LCR shedding frequency. The range of LCR shedding periods was found to be 6 to 17 months, with an average of 11 +/- 3 months. LCRs were most often observed to separate from the LC in spring/summer, with fewer LCR separations in the fall and winter months.

Hamilton et al. (1999) used satellite SST, surface drifters, and hydrographic surveys to look at ten LCRs between 1985 and 1995. They seeded the LCR with drifters, and returned periodically with shipboard surveys. The LCR pathways did not show a preferred latitudinal trend, and there was furthermore no north-south preferred direction for the LCRs to drift after they arrived at the western GOM continental slope.

Oey et al. (2005a), in their review article summarizing observational and numerical model progress in studying the GOM circulation over three decades of research, gave a summary of what is quantitatively known about LCRs, stating that they shed from the LC at a frequency of once every 3 to 17 months, are 200-300 km in diameter and 1000 m depth, have swirl speeds of 180 to 200 cm/s (similar to the LC), and westward translational speeds of 2-5 km/day, with lifetimes of several months to 1 year.

C. The northward extension of the LC and the LCR separation process

The northward penetration of the LC has also received focused study. Sturges and Evans (1983) analyzed a 13-year time series of the north-south position of the LC, and found it to be correlated with sea level and geostrophic currents at the coast (St. Petersburg and Key West, FL). They found a wide range of time periods (8 to 30 months) for the LC/LCR shedding cycle, and hypothesized that wind forcing may be setting the frequency. Further upstream, Candela et al. (2002) used a 2-year-long array of eight current meters from 2000-2001 in the Yucatan Channel to examine the correlation between vorticity flux in the Yucatan Current and the evolution of the LC in the GOM, specifically finding a correlation of the vorticity flux with the northward LC extension and LCR shedding.

Relevant to the 2010 DWH oil spill scenario, Huh et al. (1981), using shipboard and aircraft data from platforms that were in the area on another mission as well as satellite SST imagery, observed an unusual event in February 1977 where the northward extension of the LC penetrated far north onto the Florida panhandle shelf over De Soto Canyon, reaching a distance of only 8 km from the shoreline. This clearly demonstrates the possibility for a direct and rapid connection between the far northern central GOM and the downstream path of the LC system and south Florida coastal waters.

Forristall et al. (1992) used AXBTs and AXCPs plus shipboard surveys conducted during May through August 1985 to describe the most well-studied but also the most unusual LC/LCR separation event to date. The LC became very elongated to the west prior to the LCR shedding. They documented that there was a closed circulation in the LC/LCR before the LCR had completely separated from the LC. After the LCR separated it quickly split into two eddies (named "Fast Eddy" and "Ghost Eddy"). They noted that this may have been the only time that this strange event producing two simultaneous LCRs had ever been observed.

Sturges et al. (1993) provided the first detailed use of a numerical model to study the GOM circulation, primarily the LC/LCR shedding process. Using a 12-layer primitive equation model, they found that the period of time that it took for a LCR to fully separate from the LC was on the order of 30 weeks, and that it involved many weeks of recirculation between the LC and the LCR with several near separations and reattachment episodes. It should be noted that this was also the first modeling study to resolve the vertical structure of the currents in the GOM, and the first to use realistic sill depths for the Yucatan Channel and the Florida Straits.

Vukovich (1995) generated a 17-year data set on the monthly average distance between the northern boundary of the LC and 30^{o}N, and found that the northern excursion of the LC occurred on about the same frequency as the LCR shedding, with an average of 11.1 months. Sturges and Leben (2000) examined all LCRs since 1973, a total of thirty-four. Incorporating satellite altimetry, which became available in 1992, allowed them to have satellite data that was useful during the summer months and was uncontaminated by cloud cover, unlike satellite SST in the Gulf. They noted that with this analysis the ambiguity as to whether a LCR had separated from the LC or not had been reduced but not eliminated. Similar to previous work, they found primary peaks in LCR separation to occur at intervals of 6 and 11 months, and felt that incorporating altimetry allowed for more accuracy in this estimate.

D. Cyclonic eddies

Cyclonic eddies, of sizes ranging from the small frontal eddies along the edges of the LC and LCR to larger cyclonic eddies nearly the size of LCRs, are also significant to the GOM circulation and may indeed play an important role in the LCR shedding process. First noted by Nowlin and McLellan (1967) and Cochrane (1972), these cyclonic eddies were studied more quantitatively by Paluszkiewicz et al. (1983) who observed a frontal eddy intrusion onto the shelf using cruise data and satellite SST imagery and examined the role of LC frontal eddies in upwelling, mixing, and other boundary processes contributing to local modification of GOM water masses.

Vukovich and Maul (1985) provided a quantitative analysis of the cyclonic eddies on the edge of the LC, finding that their velocities were >100 cm/s and their diameters were on the order of 80-120 km. They further noted that cyclonic eddies located on the east side of the LC, i.e. along the southwest Florida shelf, always preceded LCR separation events. Oey et al. (2005) described cyclones and frontal eddies as being 50-150 km in diameter, and extending to 1000 m depth, similar to the LC and LCRs.

Later, using a numerical model initialized with satellite SST and altimetry and verified successfully with drifter data, Oey et al. (2005) showed the importance of the cyclonic eddies and noted that they can interact with and affect the LC and LCR, making the complex system challenging to describe, understand, and predict. The model predictability was assessed to be only 3-4 weeks, which is particularly relevant to the problem of the DWH oil spill and whether the oil could spread to south Florida via a direct or indirect path.

Zaval-Hidalgo et al. (2006) used satellite SST, sea surface height (SSH), and a numerical model to show a correlation between the presence of large cyclonic eddies north of the LC northward extension and an increase in the time it takes for a LCR to separate. They speculated that the presence of a cyclonic eddy to the north delays the northward extension of the LC. They described such an event that occurred in 1998, when at the same time the largest cyclonic eddy that had ever been observed with satellite altimetry was located north of the LC extension, and at the same time the largest period between LCR shedding events was observed since 1973.

E. Water masses in the GOM

Water mass analysis is an enlightening tool to use in understanding the circulation of the GOM. Nowlin and McLellan (1967) provided one of the first looks at this topic, describing the TS structures in the GOM and Florida Straits. They noted that the GOM hydrographic conditions were nearly uniform below 17^{o}C, and described the surface water dispersal of the Mississippi River water in the northern Gulf. Using additional shipboard data, Nowlin (1972) further examined the water mass distribution in the GOM and described the surface water, the subtropical underwater (SUW) in the LC and LCR, the oxygen minimum, the Antarctic Intermediate Water (AAIW), and the North Atlantic Deep Water (NADW) signals.

Schroeder et al. (1974) provided a more comprehensive description of the water masses in the GOM and Florida Straits, also from shipboard observations. Using TS analysis, they divided the water masses into three types: uniform deep water, inflowing Caribbean water containing high salinity maximum SUW, and Gulf water having a fresher salinity maximum in the same density range due to mixing and the addition of fresh water (from river discharge and precipitation) to the GOM. The observed spatial variability in the surface mixed layer was attributed to spatial differences in local inflow and runoff conditions. Schroeder et al. (1974)'s observations were focused on the LC, one older LCR, and one newer LCR. Paluszkiewicz et al. (1983) refined the previous analysis and identified three water mass types, LCW (Loop Current Water, having a high salinity maximum), CEW (coastal edge water, cooler and fresher than LCW), and shelf water. They also described interleaving TS structures between the LCW and the CEW.

F. Circulation in the western Gulf

Brooks and Legeckis (1982) used shipboard data and satellite imagery from April 1980 to examine the hydrographic features in the far western GOM, documenting a southern anticyclonic feature and a northern cyclonic feature, with entrainment of relatively cooler and fresher waters from the Texas shelf observed in the cyclonic eddy. They observed that the anticyclonic eddy contained higher salinity SUW, and based on this they hypothesized that it had a LC/LCR origin. Subsequently, Brooks (1984) used an array of current meters in the western Gulf to show that the currents over the northwest GOM continental slope are dominated by the passage of LCRs. They found only a marginal correlation with the winds, except during the passage of hurricanes, and noted that tidal variability accounted for only 1% of the total variance. Brooks (1984)'s major conclusion was that LCRs cause most of the current and hydrographic variability in the western Gulf, and that with modern remote sensing techniques there was potential for them to be identified, tracked, and to some degree predicted.

G. Circulation on the southwest Florida shelf

Sturges and Evans (1983) described the west Florida shelf circulation and how it is forced to a large extent by the southward-flowing LC. They showed that sea level at the coast is a good indicator of the predominantly geostrophic coastal currents, which flow on average at 10-20 cm/s to the south. Hetland et al. (1999) used a numerical model to further show that a pressure gradient imposed upon the west Florida shelf by the LC causes a southward-flowing jet along the shelf edge. They confirmed this modeling result with satellite altimetry and surface drifter trajectories during 1996-1997. They note that the exception to this process occurs when the LC is in its "youngest" phase, i.e. when it has recently shed a LCR and is not extended to the north in the Gulf. During these conditions, the shelf edge jet becomes diffuse over the entire west Florida shelf region.

Meyers et al. (2001) used an array of five current meters deployed on the west Florida shelf and shelf break at 30 to 300 m water depth during 1995-1996 to examine the local velocity structure and its temporal evolution. Their results were that the flow was as often northward (up to 70 cm/s) as southward (up to 120 cm/s, forced by proximity to the LC). They noted that extreme current reversals (in one case on the order of 100 cm/s within a few days) were observed in the records. There were a total of three strong southward-flowing events driven by the LC observed in the year-long record.

H. Circulation on the northern GOM shelf

Nowlin and McLellan (1967) and Nowlin (1972) first noted the variability in the northern GOM circulation with regard to the spreading of the Mississippi River discharge. They found that the circulation there was generally westward, but that there could be a seasonal influence in which there is a positive correlation between times of more Mississippi River discharge and westward flow (in the summer) as opposed to eastward flow when there was less river outflow (during the winter), but noted that there appeared to be a great deal of variability to this.

Wiseman and Dinnel (1988) used a vertical array of 4 current meters deployed near the Mississippi River delta during 1984-1985 and found less of a seasonality in that most of the current variability at that location was due to northern intrusions of the LC, and that otherwise the current variability was minimal. Morey et al. (2003) used a numerical model and surface drifters to further examine river discharge pathways in the northern GOM. They discussed the importance of the annual cycle of wind stress, which drives the fresh water discharge to the east in the spring/summer, where it can be transported offshore by mesoscale eddies, and westward in the fall/winter, where it flows south along the Mexican shoreline as a coastally-trapped wave. [THIS IS CONTRADICTORY WITH NOWLIN'S RESULT - NEEDS TO BE CHECKED.]

I. Deep currents in the GOM

Molinari and Mayer (1982) provided some of the first direct measurements of the deep flow in the GOM. They used current meter observations located at two sites on the continental slope of the eastern GOM, offshore of Mobile, AL and Tampa, FL in water depths of approximately 1000 m. They found that at the bottom (moored instruments at approximately 940 m depth) the mean flow was fairly weak (1.5 to 2.5 cm/s) and tended to be aligned with the bottom topography, northward offshore Tampa and westward offshore Mobile. Coincidentally, the Mobile site was located over the De Soto Canyon, adjacent to the Mississippi Canyon and close to the DWH oil spill location.

Their observations were later reviewed and augmented by Hamilton (1990), who made a more comprehensive study of the deep (1000 m) eastern, central, and western GOM circulation. They found mean velocities to be small and to form a large cyclonic gyre comprised of northward flow along the west Florida continental slope, westward flow along the northern Gulf, and southward flow in the western GOM along the Mexico slope. Mean velocity magnitudes were on the order of 2 to 3 cm/s.

Hofmann and Worley (1986) used hydrographic data and inverse methods (utilizing the concepts of mass conservation and geostrophy) to determine a level of no motion (LONM) in the Gulf and solve for the geostrophic circulation as a three-layer system. The best LONM was found to be at the bottom of the AAIW layer at approximately 800 to 1000 m depth. They noted that although the method was a success, yielding realistic inflow and outflow transports for the Yucatan Current and the Florida Current, respectively, it could have been improved if they had incorporated more and better hydrographic tracer data into the analysis. It should be noted that, later, DeHaan and Sturges (2005) furthered the understanding of a deep mean cyclonic circulation underlying the upper 1000 m primarily anticyclonic GOM circulation dominated by the LC and LCRs, using historic current meter data as well as profiling PALACE floats at 900 m depth, and confirmed that a LONM at about 1000 m gave a surprisingly accurate velocity result for both the upper and deeper layers of the circulation.

Finally, Sturges and Kenyon (2008) used long-term wind and current data sets (including ship drift data) to describe the presence of a net mean upper layer westward surface flow over the central Gulf as requiring vertical motion (i.e. down-welling) to balance the westward flow, and speculate that the down-welled deep flow then exits the GOM via the Yucatan Channel and/or the Florida Straits. They point out that there is observational evidence in the water mass signatures of the Yucatan Current to prove that the salinity of the AAIW coming in to the GOM is lower than that of the same density layer flowing out of the GOM at depth, which supports their down-welling hypothesis.

3. Data and Methods.

A. Hydrographic Survey

Shipboard sampling was performed using an interdisciplinary suite of instruments. Conductivity-Temperature-Depth (CTD) casts were conducted from the surface to 2000 m. These CTD casts were performed utilizing a Sea-Bird Electronics (SBE) 9*plus* CTD, ~~configured with~~configured with dual temperature (SBE 3), conductivity (SBE 4), and oxygen sensors (SBE 43), chlorophyll *a* (chl_a) and ~~Colored~~ Chromophoric Dissolved Organic Matter (CDOM) fluorometers (both WET Labs ECO FL), and a 24-Niskin bottle water sampler. Two (upward and downward-looking) internally-logging, Teledyne RD Instruments 300 kHz Lowered Acoustic Doppler Current Profilers (LADCP) were also attached to the CTD frame. In addition to temperature profiles recorded during CTD casts, the upper ocean thermal structure was measured using Sippican *Deep Blue* eXpendable BathyThermographs (XBT), which produced temperature profiles from the surface to 850 m. Continuous underway measurements of sea surface temperature, salinity, chl_a, and CDOM were collected using the onboard flow-through seawater system, which was equipped with an SBE 21 thermosalinograph (TSG) and Seapoint chlorophyll and CDOM fluorometers. Continuous measurements of upper ocean current velocity were also recorded using a Teledyne RD Instruments 150 kHz hull-mounted (or Shipboard) Acoustic Doppler Current Profiler (SADCP).

Icthyoplankton sampling, targeting larval pelagic species such as tuna and billfish, was performed with surface and profiling nets. These net tows simultaneously sampled for tar balls and weathered oil (See subsection B below). Surface net tows, including Spanish bongo (505 µm mesh), Spanish neuston (505 µm mesh), and standard neuston (947 µm mesh) net tows, were towed for 10 minutes at an average speed of 1 m s^{-1}. Though considered a surface tow, *Spanish* bongo and neuston tows were cycled between the surface and a depth of 10 m ten times during each tow. The MOCNESS ~~was~~ had a $1m^2$ frame ~~of $1m^2$~~, was equipped with 5 nets (505 µm mesh) and towed at a speed of 1 m s^{-1}. The system was typically lowered at 7-10 m min^{-1} (net 0) and hauled in at 5-7 m min^{-1} (nets 1-4). It sampled depths of 0-100 m, 100-75 m, 75-50 m, 50-25 m, and 25-0 m (nets 0 through 4, respectively). Neuston nets were 1 X 2m frame opening, slightly larger than used by Atwood et al. (1987) and Joyce (1998, per. Comm.).~~Surface and profiling tows were also utilized in the search for tar balls (see subsection B below).~~

The shipboard survey included 15 transects (labeled A-O in Figure 3) conducted during two legs (Leg I: Miami to St. Petersburg, FL from June 30 through July 12; and Leg II: St. Petersburg to Pascagoula, MS from July 13 through July 18). The sampling strategy (including both cruise track and sampling locations) was continuously updated throughout the cruise, based upon the location of predominant GOM mesoscale circulation features such as the LC, LCRs, and cyclonic eddies. The feature locations were determined from analysis of collected *in situ* data and a review of daily remotely-sensed products such as satellite-derived fields of geostrophic surface currents. For the entire 19-day survey, section coverage totaled approximately 3000 km. A total of 73 stations were occupied and sampled with lowered equipment, 191 XBT profiles were collected, and 24 satellite-tracked Lagrangian drifting buoys, drogued to follow the water at a depth of 15 m, were deployed.

Water property and velocity measurements collected along occupied sections (Figure 3) were analyzed to assess the vertical and horizontal structure of the mesoscale circulation features observed and to characterize the physical connectivity between features. CTD potential temperature-salinity (θ-S) profiles were grouped by similarity to one of three prototypical GOM water type θ-S signatures (over a density range from $\sigma_\theta = 24.0$ kg m^{-3} to $\sigma_\theta = 26.5$ kg m^{-3}, as defined in Table 1). Selected from CTD station data collected during this survey, the three prototype θ-S profiles were identified as GOM Common Water (GCW), Loop Current Water (LCW), and Eddy Franklin Core Water (EFCW). These prototypes (shown in Figure 4) were selected based upon historical GOM water mass literature (c.f. Nowlin and McLellan 1967; Nowlin 1972; Schroeder et al. 1974; Paluszkiewicz et al. 1983). There is some ambiguity in the water mass naming conventions used in the literature. For the purposes of this study we will use the following water mass classification: θ-S profiles with a structure indicative of an interleaved or mixed combination of the three prototypes will be classified as "mixed", profiles significantly fresher than GCW will be labeled Coastal Shelf Water (CSW), and profiles not reaching a density of $\sigma_\theta = 24.0$ kg m^{-3} will remain "unclassified". The spatial distribution of these groupings will be discussed in Section 4.

The LC, and the anticyclonic LCRs which it periodically sheds, both share a characteristic deep layer of high salinity associated with SUW which is formed in the Atlantic Ocean, and delivered to the GOM via the Caribbean and Yucatan Currents (Nowlin 1972; Schroeder et al. 1974; Paluszkiewicz et al. 1983). In some cases, separated LC eddies and water recirculating within the center of an elongated, but still attached, LC may develop a unique θ-S relation, differentiating these features from the main LC. This can occur when these anticyclonic bodies are exposed to wind-driven mixing and the development of a deep mixed layer in winter months, followed by summertime heating and the restoration of a seasonal thermocline (Paluszkiewicz et al. 1983). The resulting θ-S profile yields a region of constant salinity and decreasing temperature in the upper water column, above the characteristic LC deep salinity maximum. In the case of EF, this was observed to a depth of 130 m and clearly distinguishes the EFCW prototype (yellow) from the LCW prototype (magenta) in Figure 4.

Unlike waters more recently arrived from the Caribbean, the GCW θ-S relationship is characterized by greatly diminished subsurface salinity maximum (cyan prototype in Figure 4). This signature is a result of mixing, driven by frontal passages crossing the region, with surface freshwater inputs along the GOM coastal shelf (Nowlin 1972; Paluszkiewicz et al. 1983).

The continuous records of GoM surface salinity, chl_a, and CDOM, recorded by the shipboard flow-through TSG and fluorometers at 1-minute intervals, were linearly interpolated to a standard distance interval of ~~X~~ 0.25 km along the cruise track. This interpolation removes artifacts caused by over-sampling when the ship stops or reduces speed. T~~T~~he ~~resulting~~ data were ~~then~~ grouped according to the nearest θ-S profile classification and analyzed to determine if there were significant differences in the biogeochemical surface data among the water masses to further support a lack of direct connection among these groupings.~~. [Chris, you can put more here, but we should probably come back to this in Section 4 rather than elaborating here. I think the basic gist will be that the surface waters are highly variable across the spatial extent of our survey, supporting our rationale for the need to analyze the water over a density range with the θ-S profile analysis, and the need for in situ water column obs and not just surface measurements alone [Ryan]~~. ~~IT WILL BE GREAT TO HAVE A LINK BETWEEN THE θ-S RELATIONSHIPS AND THE CHEMICAL DATA.~~

B. Surface and Subsurface Oil Observations

Methods for observing surface oil and tar balls over the survey region included visual observations of the sea surface during daylight hours, net tows, and the flow-through CDOM fluorometer. Bow observers were on watch during all daylight hours, recording the number and condition of seabirds for a separate research study, and reporting any observations of surface oil or tar balls to the Chief Scientist.

WE NEED LANGUAGE ON VISUAL OBSERVATIONS, HOW MANY HOURS A DAY THIS WAS DONE, WHAT TYPE OF FINDINGS ONE USUALLY GET FROM DOING THIS, ETC..,Ryan needs to add this, as he was the Chief Scientist… or at least verify this…I think I have written what he told me about what was done, but you need to check.

Following each net tow, nets and net frames were carefully examined by eye for the presence of tar balls. ~~. [CAN WE ADD LANGUAGE ON WHAT SIZE OF TAR BALLS THESE NETS COULD HAVE FOUND, IF THIS IS A STANDARD PROCEDURE, ETC]~~ ~~**[mesh sizes of the nets were already previously defined, I think Michelle had some literature on tar ball sampling procedures prior to the DWH spill – we could compare and contrast our methods with historical methods here, or it could be discussed in the results and discussion – Ryan]**~~The Neuston nets used for this work should have permitted capture of tar balls and semi-solid masses of weathered oil <1mm in diameter; other nets used onboard would have captured even smaller particles (~0.5mm). Both Bongo and Neuston nets are light in color, permitting easy detection of tar balls if they are present; the nets for the MOCNESS are dark in color and so presented more potential opportunity for small tar balls to be missed during visual inspection of the nets.

The search for oil and hydrocarbon contaminants within the water column relied upon two types of measurements. Data from the CTD dual SBE 43 dissolved oxygen sensors were utilized as an indirect proxy for subsurface oil, as microbial degradation of oil or accompanying methane within the water column could intensify oxygen depletion (Kessler et al. 2011; Joye et al. 2011). Additionally the CTD WET Labs ECO FL CDOM fluorometer was ~~used in an attempt~~ to detect the fluorescence of ~~subsurface spill contaminants. [IS THIS CONSIDERED DIRECT OR INDIRECT MEASUREMEN~~oil in subsurface layers as was commonly being done during the spill response (c.f. Diercks et al. 2010)~~T~~?]

Crude oil is a combination of hydrocarbon components that, as a mixture, typically fluoresce strongly when excited in the blue spectrum at wavelengths below 300 nm, and may emit broadly from 300 nm up through the red past 600 nm (Green et al. 1983). When trying to measure hydrocarbons from a specific source by optical means, ideally a fluorometer would be tuned to the precise excitation (EX) wavelength which yields a maximum emission (EM) wavelength. Following standardization with source material, such an instrument could then be calibrated to report a first order estimate of source specific oil concentration. To employ such a fluorometer in the “search” for subsurface oil, one would optimally utilize the sensor by recording continuous measurements, either as part of a ship’s flow-through system (yielding continuous measurements at the sea surface along the ship track), or as part of a lowered CTD instrument package (yielding continuous measurements from the surface to a maximum cast depth) so that a survey could direct sampling efforts based on the sensor data in real-time. However, this scenario assumes the optical properties of the target oil to be stable. We know this not to be the case, as dispersal and/or the natural weathering of crude oil will change its fluorometric response (Henry et al. 1999). Additionally, variability in the unique chemistry of different source oil targets will result in fundamental EX/EM property differences between targets (Bugden et al. 2008). Given these complexities, ~~the use of *in situ* fluorometers should be combined with periodic sampling when quantifying oil distributions (Henry et al. 1999). [SHOULD THIS LAST SENTENCE BELONG IN THE CONCLUSIONS?] MICHELLE: CAN YOU PROVIDE SOME LANGUAGE ON A QUANTITATIVE ANALYSIS. THE TEXT ABOVE IS GREAT AND TELLS ME HOW TO POTENTIAL FIND OIL. NOW, HOW DO~~we note that the flourometers we used are fixed wavelength fluorometers that

~~WE KNOW IF WE HAVE FOUND A LITTE, SOME, OR A LOT OF OIL ?]~~

~~At the time of the July 2010 survey, a tuneable wavelength fluorometer was not available, nor was a multi-channel fluorometer suitable for sampling a combination of EX/EM wavelengths. Thus, the previously mentioned CDOM fluorometers were utilized. These fixed wavelength fluorometers~~ were not specifically designed to measure hydrocarbon concentrations, as their EX/EM ranges (WET Labs ECO: 350 nm EX / 430 nm EM; Seapoint: 370 nm EX / 440 nm EM), while within the crude oil range, were selected for the detection of CDOM (a naturally occurring material, heavily concentrated in coastal areas). A CDOM fluorescence peak, identified using a similar WET Labs ECO fluorometer, was detected early in the spill near the MC252 wellhead at depths >1000 m and was confirmed to be due to the presence of hydrocarbons (Diercks et al. 2010). Additionally, Wet Labs provided preliminary data indicating that the ECO CDOM fluorometer was sensitive to the presence of hydrocarbons. Therefore, both fluorometers were utilized as preliminary indicators for the possible presence of hydrocarbons and to target sample collection. However, use of ~~a fluorometer~~a fluorometer that could detect fluorescence in the UV might have identified subsurface oil at lower concentrations than we could detect with the instruments we used.

C. Satellite-derived Observations

Synoptic observation of the earth surface conducted over large geographic areas is a key advantage of utilizing satellite-mounted environmental sensors. Earth observation satellites associated with the NOAA Polar-orbiting Operational Environmental Satellite system (POES) system and the NASA Earth Observation System (EOS), are capable of acquiring visible and infrared data over large geographic areas, while providing frequent and repetitive coverage. These sensors, together with altimeter data, were essential in the delineation of surface oil, especially under sun-glint conditions. On board sensor type and orbit characteristics determine spatial, spectral and radiometric resolutions, which are closely related to the data volume received by satellite ground stations. Today, many satellite products are available in near real-time, and consequently, greatly contribute to the development of operational oceanography programs. During the DWH oil spill incident, ocean conditions in the GOM were intensively monitored using data from multiple satellite sources, which provided on a continuous basis essential information about the status and distribution of spilled oil, complementing *in situ* observations and becoming critical assets for decision making.

Horizontal gradients of SSH fields derived from satellite altimetry were used to estimate daily surface geostrophic currents and, from their spatial gradients, to determine the locations of the fronts associated with the cyclonic and anticyclonic features such as LCRs and eddies (Figures. 1, 5, 6a, 6c, 6e, and 6g). These surface current fields reveal the dynamics at the ocean surface, and have the advantage of a basin-wide coverage. ~~However, a~~Although they have the benefit of not being subject to cloud contamination, they cannot provide the fine spatial resolution of satellite-derived maps of SST. In addition, surface current fields are detectable year-round and are not affected by the uniform SST values often observed over the Gulf in summer months.

Since altimetry fields are constructed using the "alongtrack" satellite data, which may not necessarily run along or across the region of LCR detachment, the exact date of detachment as seen from SSH observations is only approximate. Results regarding the separation of the LCR from the LC, based on surface currents alone, may also differ from that obtained from SST estimates, as the mesoscale feature derived from dynamic and temperature fields may not necessarily coincide. Additionally, separation at the surface and separation at depth usually occurs at different times (Nowlin and Hubertz 1972; Forristall et al. 1992; Sturges et al. 1993), with separation at depth only verifiable via *in situ* measurements. It is also important to note that for a region such as the GOM, satellite altimetry produces a synoptic field of currents. Due to the extent of the coverage area, the same cannot be said for *in situ* current velocity measurements collected by a research vessel.

Besides altimetry, SST fields from AVHRR, MODIS and ENVISAT's ATSR, and ocean color fields obtained from MODIS, SeaWiFS and MERIS were also used to identify the dynamic features in the Gulf during the incident. Absolute and relative values of these parameters can be associated with changes in the water properties and transports in the region. The location and extent of these ocean features can be continuously monitored using data from the sensors mentioned above, which although they are affected by clouds, provide repetitive and synoptic coverage over the region, near real-time data availability and validated/calibrated products.

At the same time, the NOAA/NESDIS Satellite Analysis Branch (SAB) were creating operational satellite derived oil analysis using as main inputs high resolution data from SAR, MODIS (~250 m) and MERIS (~300 m) sensors. In some rare cases during the event, and when high resolution data were not available or did not provide useful information, AVHRR 1 km resolution imagery was used. The main purpose of these analyses, which were routinely sent to the NOAA Office of Response and Restoration (ORR), the U.S. Coast Guard, and the Minerals Management Service, was to delineate the extent of the oil on the ocean's surface, with its potentially huge implications for decision making activities during the crisis. Contrary to what was required from visible and near infrared satellite data to estimate geophysical parameters, optimum conditions for oil detection using MODIS and MERIS data greatly benefit from the presence of sun-glint [REF?].

D. Surface Drifter Observations

Satellite-tracked surface drifters were used to estimate the Lagrangian pathways of near-surface water that had traveled near the site of the DWH oil spill. These drifters are styled after drifters developed in the Surface Velocity Program (SVP) and are drogued at a depth of 15 m, to minimize direct wind forcing (Lumpkin and Pazos 2006), and thus, they potentially represent the motion of water in the ocean mixed layer rather than the motion of oil floating at the surface.

During June and July 2010, the NOAA Global Drifter Program (GDP) coordinated the deployment of 36 SVP surface drifters in the LC system, 12 from the University of Miami's R/V *Walton Smith* on June 7-9, along a transect from Louisiana to South Florida, and 24 from the NOAA Ship *Nancy Foster* during the cruise documented here. A number of additional shallow water CODE (Coastal Ocean Dynamics Experiment) style drifters were also deployed by other agencies including the University of South Florida, Horizon Marine, and the US Coast Guard; the CODE drifters are not analyzed here. The purpose of the drifter deployments was to provide *in situ* measurements of near-surface currents, and to provide pseudo-Lagrangian tracking devices to follow water in the region of the oil spill.

4. Results and Analysis

A. Pre-Cruise (April through June) GOM Assessment

The thermal structure and dynamic conditions present in the GOM during the summer of 2010 were typical for the basin and time of year. SSH and SST values were only slightly lower than average (http://www.aoml.noaa.gov/phod/dhos/geos.php). However, as altimetry-derived surface fields for the GOM shown in Figures 1 and 5 emphasize, a high level of variability existed in the location and size of GOM mesoscale features during the period.

The surface conditions observed between April and May 2010 indicated that the LC extended to ~27°N in the longitude range 85-88°W. During May and June 2010, satellite observations documented the initial separation of the anticyclonic EF from the LC and the subsequent interaction of these features with one another (including reattachment of the outer edge of EF in the second half of June). While this LCR separation may have inhibited direct connectivity between northern Gulf regions and downstream areas, synthetic drifter trajectories obtained from numerical models using model and satellite-derived ocean current fields indicated that water particles could still travel from the oil spill site into the southern GOM. EF remained in a state of partial attachment/detachment during June (Figures 1d and 1e). It was hypothesized that during June 2010 the cyclonic eddies situated between the MC252 wellhead and EF (blue contours in Figures 1c through 1i) had the potential to disperse surface and subsurface oil into the rest of the GOM. In fact, tar balls sourced to MC252 were observed along the eastern border of EF on June 8, 2010 as far south and east as 26°45.85'N, 086°03.65'W [show in panel 1d or 1e] **[okay, I will – Ryan]**(~~A. M. Wood, WS1010A mission report, in preparation~~NOAA Factsheet, Walton Smith June 6-10 Cruise Report/ http://www.noaa.gov/deepwaterhorizon/publications_factsheets/index.html#list; Wood et al., In prep.).

By the end of June, the cyclonic features located on both sides of the EF/LC region of attachment served to zonally elongate the connection between the reattached EF and LC, resulting in a westward translation of EF and what appeared to be a second separation (Figure 1f). Concurrently, the main LC remained in essentially the same location flowing northeastward towards the west Florida shelf before turning towards the southeast and entering the Florida Straits. Despite the separation, reattachment, separation scenario indicated by satellite observations, the level of connectivity between EF and the LC during the month of June was somewhat ambiguous. Four of the surface drifters deployed from the R/V *Walton Smith* in early June (near 26°N and 84°W) moved southwestward, cutting across streamlines derived from altimetry (Fig. 1e) on 14-16 June and suggesting that EF had not reattached and had possibly remained disconnected since the beginning of the month (Figure 1d).

~~THIS GOM ASSESSMENT IS FOR CIRCULATION ONLY. WE NEED TO STATE HOW THE SURFACE OIL SPREAD AND CHANGED DURING THIS PERIOD, IF NOT, WE NEED TO CHANGE THE NAME OF THIS SECTION TO SOMETHING LIKE "PRE CRUISE GOM CIRCULATION~~The offshore location of the well meant that oil reaching the surface had considerable opportunity for dispersal by local currents and wind. Much of the movement of surface oil was to the north and northwest~~, threatening~~, threatening the coastline.

However, there was also offshore movement ~~of oil~~of oil that became associated with southward and southwestard flow in the convergence of a counter-clockwise eddy nearly centered at the well-head, and a counterclockwise eddy to the SW. By May 15, this oil had been entrained into the northern edge of the counter-clockwise flow of the feature that would become EF (Fig. 1). As EF drifted south in late May and early June, the apparent connectivity to sources of new oil from the well head was broken (Fig.1) although some filaments of surface oil ~~extending toward~~extending toward EF still appeared in surface oil projections provided by NOAA's Office of Response and Restoration as late as June 1 (Fig. 1), at which point EF appeared to be separated from the LC and was thought to be a possible 'reservoir' for floating tar balls and surface oil that was weathering in place. The apparent separation of EF from the LC suggested that any surface oil that had moved away from the wellhead towards the Florida Straights was actually restrained in EF, and the LC protected from accumulating oil by this large retentive feature (Fig. 1). ”~~.~~

B. GOM Circulation in the far field, July 2010

With the level of connectivity between EF and the LC questionable over June 2010, even at the surface, where remotely-sensed and drifter observations provided data coverage, concerns continued to mount regarding the potential for delivery of DHW contaminants to downstream ecosystems adjacent to the Florida Straits. In this environment, the July research cruise, conducted aboard the NOAA Ship *Nancy Foster*, supplied needed surface and subsurface information regarding the connectivity between these two features.

SADCP surface current measurements collected during the cruise revealed similar surface circulation features to those derived from satellite altimetry (which were utilized to guide the survey). Comparisons between these two methods are shown for four highlighted sections in Figure 6 as a validation of the altimetry-derived surface velocity estimates at different stages of the cruise over the survey region (Figure 6a, 6c, 6e, and 6g). Surface velocity fields from both sources were utilized in conjunction with CTD/ADCP hydrography to parameterize the separation and/or connectivity between the observed mesoscale features.

As previously described in Section 3, θ-S profiles were binned according to their similarity to prototypical CTD θ-S signatures associated with GOM water masses and circulation features (Figure 4, Table 1). The spatial distribution of the θ-S signature groupings observed across the survey region (Figure 7) shows the relative location of each signature type in relation to the maximum recorded surface velocity associated with each eddy feature and illustrates how these flows can act as a barrier to mixing within the eddy core, and at the same time, entrain water and promote mixing between the velocity maximum and the circulation front. CTD station location markers are color coded by θ-S grouping and plotted atop SADCP velocity vectors in Figure 7.

The altimetry-derived surface currents corresponding to July 7, 2010, covering Section E (highlighted in Figure 6a), have excellent quantitative and qualitative agreement with the SADCP surface velocities and SVP drifter trajectories originating along this transect.[RYAN, JOAQUIN, CAN WE PROVIDE ESTIMATES OF THE ACTUAL VALUES OF THE CURRENTS ?]**[YES, BUT THE ADCP VELOCITIES ARE MORE OR LESS INSTANTANEOUS (A FINAL PROFILE EVERY 5 MINUTES), THE ALTIMETRY VELOCITIES ARE A COMPOSITE CENTERED ABOUT A GIVEN DAY, AND ANY**

VALUE OFF OF A TRACK IS AN INTERPOLATION BETWEEN TRACKS – HOWEVER, DESPITE ALL OF THIS, THE MAX SADCP AND ALT VELOCITIES ALONG THIS LINE AGREE WITHIN 14 CM/S -RYAN] Along the eastern half of the section, observations confirmed the altimetry estimates of a northeast-flowing LC impinging upon the southwest Florida shelf break and subsequently turning southeast. Mixing of LCW with both CSW of the west Florida shelf and with GCW to the west was visible in θ-S profiles for this section, indicating the potential of an indirect pathway into the southern GOM region. The GCW observed was associated with a large cyclonic eddy located west of the LC retroflection.

The SADCP and LADCP data collected during the several crossings of this cyclonic frontal eddy revealed a surface intensified maximum velocity of of approximately 180 cm/s. This feature possessed an approximate radius of 120 km. The depth of the main thermocline, measured from both CTD/LADCP casts and densely-spaced XBT deployments over the region (Figure 3), confirmed the size and location of this cold-core cyclonic circulation. Though not evident in Section E (Figure 6b), velocity and water property sections for transects G, H, and J (Section J shown in Figure 6d) revealed a cyclonic circulation extending to at least 2000 m (the maximum depth of our CTD/LADCP casts). Deep velocities of 40-50 cm/s were observed. It is unclear if the observed deep velocities (deeper than 1000 m) were directly related to the upper-ocean, surface-intensified circulation or to some other deep GOM circulation dynamic. The location of this deep cyclonic circulation agrees with results from Hamilton (1990). However the velocity magnitudes observed during this survey were much larger**. [I STILL NEED TO INVESTIGATE THIS A LITTLE MORE – Ryan]**

The westernmost CTD/LADCP station along Section E, conducted on July 8, revealed a θ-S signature corresponding with EFCW (yellow profile/marker, Figures 4 and 7), which was markedly different from the previous stations, confirming that the section had reached the anticyclonic EF circulation, westward of the cyclonic frontal eddy. The velocity section (Figure 6b) shows this station location to be approximately 40 km west of the strongest flow recorded between these circulating features. The southward velocity propagations across this section (blue colors on the left side of Figure 6b) belong to two different features: the cyclonic eddy that lies between the LC and EF and the northern edge of the anticyclonic motion of the LC. This section crosses only the eastern portion of EF as also depicted by the satellite-derived surface velocity fields (Figure 6a). The eastern half of this section is dominated by the northward flow (red colors in Figure 6b) of the cyclonic eddy and by the LC. The eastern edge of this section shows the southward return of LC flow against and atop the southwest Florida Shelf.

Evidence of EF core circulation was observed at the western end of Section E. However, subsequent transects G-J, conducted over the following four days (July 8-12, 2010), encountered no clearly definable EF θ-S signatures, confirming the beginning of a westward translation and meridional flattening of the anticyclone documented in the altimetry fields for this period (Figure 6a and 6b). Waters circulating in the cyclonic frontal eddy separating EF from the LC primarily exhibited GCW θ-S profile characteristics. However, many stations revealed a "mixed" water column with evidence of GCW and LCW θ-S signatures, suggesting mixing along frontal boundaries (Figures 4 and 7).

The continuous flow-through surface data (Salinity, chl_a, and CDOM) was highly variable in the coastal waters and stable in the central area of the Gulf of Mexico with low chl_a and CDOM fluorescence. The low and stable CDOM fluorescence reading that contained no anomalous peaks in the central GOM suggests that it did not detect surface oil along our cruise track in this region. However, the surface water properties in the northern extension of our survey near the Deepwater Horizon incident site were influenced by Mississippi River runoff. This caused a high degree of variability in all 3 properties and elevated CDOM and chlorophyll *a* fluorescence. Due to these elevated and highly variable measurements, the use of the flow-through CDOM fluorometer to detect surface oil near the incident site was not possible.

~~[Chris, add in some text about surface CDOM distribution – a note about the strong surface signals near the mouth of the Mississippi nullifying the use of the CDOM flow-through fluorometer as a surface oil proxy might be something we should mention. – REWORK THIS PARAGRAPH FOLLOWING REPROCESSING OF θ-S GROUPING / STATION CATEGORIES – ALSO, DESCRITPION OF METHOD IS NOW IN PREVIOUS SECTION]~~

The continuous flow-through data, binned ~~spatially by the locations of the~~by θ-S profile groupings (Figure 7), revealed that all surface water properties were significantly different among these groupings (Kruskal-Wallis ANOVA, $p<0.001$) further supporting the lack of direct connection among the water masses. Moreover, a Mann-Whitney U-test ($p<0.001$) calculated higher salinity and lower chlorophyll *a* and CDOM fluorescence in EFCW than LCW (Table 2). This suggests the surface separation of these two features was great enough to allow for distinct biogeochemical signatures likely a result of a long residence time within EF isolating the seawater from terrestrial sources of freshwater and nutrients. This would reduce chlorophyll *a* biomass due to exhaustion of existing surface water nutrient stocks, increase evaporative concentration of SSS, and increase degradation of CDOM. Both LCW and EFCW have more stable surface water properties than CSW and GCW. ~~at the sea surface, regions covered by Coastal Shelf Water (~~CSW (Table 2)~~)~~ had the lowest median salinity with the highest salinity variability and the highest median ~~chl_a~~ chl_a and CDOM fluorometry ~~(Table 2)~~. This reflects the relatively large influence of coastal processes including riverine input into these near-shore environments (Nowlin and McLellan 1967; Nowlin 1972; Schroeder et al. 1974; Brooks and Legeckis 1982; Paluszkiewicz et al. 1983; Morey et al. 2003). ~~Areas occupied with~~ GCW had the second most variable sea surface salinity (SSS), though the median SSS was still higher than that observed for LCW. The relatively large variability in SSS and surface chl_a likely reflects the proximity and interaction of GCW to continental shelf boundaries and nearshore GCW. ~~LCW was much more homogeneous at the surface with respect to both salinity and chl_a. The surface waters of EF had the highest median salinity and lowest chl_a concentration of the water groupings, with low variability in each. This likely reflects the long residence time within EF which allowed for isolation of the seawater from terrestrial sources of freshwater and nutrients. The high SSS was high due to a lack of freshwater and the result of evaporative concentration affecting the feature. Likewise, surface chl_a was low due to the lack of nutrient inputs and the exhaustion of existing surface water nutrient stocks during the extended residence time.~~ ~~**[I may need to examine the depth profiles of CDOM and CHL a from the CTD to examine differences between water masses in CDOM and chlorophyll. - CK]**~~ ~~[THIS ANALYSIS IS FINE, BUT WE NEED TO LINK IT TO THE CONNECTIVITY AND THE SEARCH FOR OIL – GG]~~

Although mixing and entrainment along frontal boundaries may have provided for an indirect pathway between EF and the LC, the features were clearly distinguishable as separate bodies indicating that a direct linkage between northern GOM regions and downstream coastal ecosystems of south Florida, northern Cuba, and the Florida Straits was no longer in place.

The observations reported herein from July 2010 clearly indicate a narrow southward jet along the shelf break (Fig. X) much like that described by Hetland et al. (1999). With the exception of this subsurface jet observed flowing parallel to the West Florida Shelf break at the eastern ends of Sections E and J (Figure 6b and 6d respectively), velocity measurements across the survey region mostly revealed mesoscale features with surface intensified flows. When considering the possible entrainment of oil initially released and dispersed at depth, which would be subsequently undergoing decomposition, there is a potential for contaminants to settle at a level of neutral density within the water column. In such a scenario, the current velocity at the corresponding depth will ultimately dictate the translation speed of the contaminant particle. In regards to the circulation features examined during this research cruise, the fastest translation speeds for entrained particles were at the sea surface. Any subsurface contaminants would have been subjected to reduced current velocities as compared with surface conditions. Additionally, using the observational methods available, no evidence of oil was observed at the surface or within the upper 2000 m water column over this region. Prior reports of a moderate burdern of pelagic tar in the Gulf of Mexico suggest that we should have seen some tar balls in our net tows (Atwood et al., 1987, Van Vleet 1983) but much of the data for these reports were collected before Annex I (oil) of the current International Convention for the Prevention of Pollution from Ships (MARPOL) went into force in 1983. Modern shipping practices may have reduced the background level of pelagic tar in the Gulf of Mexico.

~~. [MICHELLE, CAN YOU ADD A STATEMENT ABOUT HOW SOME MIGHT CONSIDER THIS WEIRD IF FOR NO OTHER REASON THAT SO MUCH OIL~~

~~NATURALLY SEEPS INTO THE GULF, THE ONE MIGHT THINK THAT WE SHOULD HAVE SEEN SOME, EVEN IF NOT FROM DWH]~~

Volume transport associated with the flow circulating about the axis of the cyclonic feature separating EF and the LC was calculated from merged LADCP and SADCP Transect G velocity section data (single crossing). The upper 2000 m transport was calculated to be 73 Sverdrups (Sv; 1 Sv ≡ $10^6 m^3 s^{-1}$). Flow in the upper 800 m comprised 35 Sv of this total (Florida Straits sill depth = 800 m). This upper 800 m volume transport is consistent with data from the highly-resolved transport time-series at 27°N in the Florida Straits (mean = 32.1 Sv, Meinen et al. 2010).

Two radial transects were conducted across EF during the survey (Sections L and M in Figure 3). Section L confirmed the elongated radius of EF of approximately 250 km. The strongest velocities associated with the anticyclonic circulation along this section were located between the surface and 200 m (surface intensified) and reached a maximum of 108 cm/s approximately 160 km from the center of circulation. EFCW θ-S signatures were observed at all CTD/LADCP stations inside of this distance. Beyond 160 km from the center, GCW was entrained in the EF circulation. Section M, conducted from the approximate center of the EF circulation to the MC 252 wellhead, revealed an eddy radius of approximately 200 km. The strongest flow observed (surface intensified velocities reaching 160 cm/s) was located 110 km from the center of the anticyclone, proportionally closer to the center of the eddy circulation. Assuming a circular ring, these velocity data suggest that particle revolution about the center of EF should take a minimum of 5 (Section M) to 11 days (Section L). However, due to the irregular shape of EF (Figures 1, 5, and 6), the ring's rotational period may be quite different. Though CTD/LADCP stations were limited along Section M due to time constraints, continuous

SADCP data collection allowed for the targeted positioning of stations on either side of this maximum velocity boundary. Water within this boundary possessed an EFCW θ-S relation, while the CTD/LADCP cast external to this boundary recorded the presence of GCW. ADCP data collected across Transect M show that circulation associated with EF appears to extend to a depth of 1120 m. [HOW ABOUT THE THETA-S ANALYSIS?] **[the portion of theta-s profiles associated with depths deeper than approximately 400 m are all identical across the different prototypes – Ryan]** The corresponding volume transport (from the surface to 1120 m) was calculated to be 42 Sv. Though the velocity section for Transect L shows weak flow at depths greater than 1120 m (Fig. 6f), it is unclear if this flow was directly associated with EF or with separate deep circulation dynamics. Continuity would suggest the latter, as the upper 1120 m volume transport for EF, calculated from velocities recorded along this section, was found to be 37 Sv (on the same order as Section M). The 5 Sv difference between these two values is likely due to the limited number of lowered velocity observations along section M and the time required to complete both transects (3.5 days). When comparing the upper 200 m transport for each section calculated from continuous SADCP velocity data (see data coverage insets on Fig. 6), the transport difference is approximately 1 Sv.

Drifter trajectories, from SVP drifters deployed within and around EF, confirmed the separation of EF from the LC over the first half of July. The drifters also revealed bifurcation points in the flow where subtle changes in location led to profound differences in downstream fate. For example, an extremely closely spaced pair of drifters at ~24°N, 84°W on July 19 moved northeast to 24.5°N, 83.5°W while slowly separating. Upon reaching 24.5°N, 83.5°W on July 22 the drifters moved in opposite directions, with the easternmost drifter entering the LC and the westernmost drifter entering the cyclonic vortex south of EF.

Throughout late July and early August, a number of drifters verified the zonal elongation of EF and the closed cyclonic eddy north of EF (Figure 1h), with few drifters passing from this feature into EF. Also starting in early August, several drifters which had been orbiting EF abruptly peeled off to the east and moved along the LC, indicating that a fraction of the eddy had reattached with the LC once again. This was also indicated by altimetry (Figure 1h 1i).

C. Near field ocean conditions, July 2010

Over the ~200 km distance between the northernmost extent of EF and the MC252 wellhead, both a low velocity cyclonic frontal eddy and an anticyclonic eddy were observed (Figure 6g and 6h). The maximum velocity observed within these flows (surface intensified) was approximately 30 cm/s. The northern interface between the cyclonic circulation and the anticyclone situated over the DWH drill site fell within the NOAA Office of Response and Restoration (NOAA/ORR) nearshore oil forecast boundary and the NOAA/NESDIS/SAB experimental surface oil coverage map(Figure 6g). *In situ* observations collected along transect M, within this oil forecast boundary, confirmed the NOAA/ORR and NOAA/NESDIS/SAB forecasts. Surface oil and tar balls were first observed approximately 84 km south of the DWH wellhead, at which time a station was conducted (station #70, location shown in Figure 7). These observations were all located north of the center of cyclonic circulation. Any entrained contaminants would therefore be carried westward prior to potential mixing along the EF front, thus lengthening the indirect pathway between the Mississippi Canyon and the prominent circulation features to the south previously described. **[I still need to add a statement about the deep flows along this line after I finish Figure 7b, the plot of deep LADCP vectors– Ryan]**

C. Surface and Subsurface Findings near MC252

On July 17, three CTD/LADCP stations were conducted at the northern terminus of Section M within 17 km of the MC252 wellhead (station #71, #72, and #73; shown in Figure 8). The location/occupation of these stations was coordinated with other survey and response vessels on site (R. H. Smith *et al.*, 2010 [NF1013, mission summary report NOAA REF]). While working in close proximity to the wellhead, intermittent surface sheens were observed. Tar balls were not visually observed at the surface while conducting these stations. However, at station #71, dark oily smudges were discovered on the 0-100 m MOCNESS net and the standard neuston net following each tow. Evidence of a subsurface hydrocarbon plume concentrated at a depth of 1155 m ($\sigma_\theta \approx 27.65$ kg m^{-3}), similar to that described by other investigators studying the spill (Camilli *et al.*, 2010; Diercks et al., 2010; Hazen *et al.*, 2010), was observed in CTD CDOM and O_2 sensor data collected at these stations (in O_2 only at station #72, Fig. 8). The strongest spikes in CDOM voltage (an increase) and in dissolved oxygen (a decrease) were observed at station #71, approximately 15 km south-southwest of the wellhead.

Total aromatic hydrocarbon concentration in samples collected from 1150 m at station #71 were estimated at 335-410 ppt from frozen samples sent to the RCAT laboratory at Louisiana State University. Total aromatic hydrocarbons observed in deep samples collected from stations #70, #72, and #73 were less than 100 ppt. Though stations #71 and #73 exhibited stronger signals associated with contaminant anomalies in both fluorescence and O_2 profiles at ~1150 m, the CTD O_2 sensors generally recorded a more gradual signal decrease (compared to the corresponding CDOM voltage increase) in O_2 concentrations near the suspected feature, over a broader depth range (between 1100 and 1400 m), resulting in a “scalloped” O_2 profile. The oxygen decrease was subsequently verified by photometric Winkler titrations performed on board. Shown in Figure 8, current velocity magnitudes in this depth range were observed to be 10-15 cm/s **RYAN - in what direction? [FIGURE 8 IS IN PROGRESS, IT WILL BE COMPLETELY REVAMPED – Ryan]**. The directionality of this deep flow may have been topographically influenced. Add a comment here regarding how the observed deep flow matches the historical mean deep flow (westward along the northern Gulf bottom topography).

5. Discussion and conclusions

In general, the hydrographic and current conditions observed during the cruise conducted during July 2010 aboard the NOAA Ship Nancy Foster agreed very well with what is known about the GOM circulation and water masses. The LC was in an elongated northward position in April 2010 at the time of the oil ~~spill which~~spill, which~~, although it~~ provides a direct pathway to the south, but is also conducive to the development of a LCR. In addition, it was surrounded by cyclonic eddies which have been shown to play an important role in the separation of LCRs from the LC.

While GOM dynamics during May and June 2010 may have provided favorable conditions for particle entrainment from the northern Gulf to the Florida Straits and bordering downstream coastal regions, remotely-sensed and *in situ* observations confirmed that, by July 2010, this was no longer the case (Figs. 1f and 1g). As the cruise progressed, the LCR designated Eddy Franklin was undergoing a lengthy process of partial separation, reattachment, and eventual full separation, but this occurred over a period of several weeks to months. The large cyclonic eddy that developed to the east of the LC and spread to the west between Eddy Franklin and the southern portion of the LC was likely instrumental in the eventual LCR separation as has been described by Vukovich and Maul (1985) and others. The separation of EF from the main LC in July and the eddy's subsequent zonal elongation inhibited direct connectivity between the Mississippi Canyon and the LC during this period. Additionally, smaller cyclonic features, located to the north and south of EF, served to lengthen any transport pathways from the drill site to the southern GOM and provided multiple opportunities for mixing *en route*.

Uncontrolled output from the MC525 wellhead was finally arrested on July 15, 2010, three days prior to the conclusion of this survey. The lack of tar balls, surface sheens, or ~~vertical~~ CDOM and O_2 profiles with signatures indicative of subsurface hydrocarbon plumes over the broad study domain (south of NOAA/ORR and NOAA/NESDIS/ SAB oil forecast boundaries) suggests that any oil carried to the southern portion of the~~the southern GOM~~ study area prior to the July survey had weathered or been dispersed to levels undetectable to our methods. While floating tar has been documented repeatedly in the Gulf of Mexico and Florida Straits (Atwood *et al.*, 1987; Joyce, 1998), as with the 1979 Ixtoc-1 spill (Romero *et al.*, 1981), there was no evidence that south Florida beaches received elevated amounts of tar as a result of the DHW spill. Most movement of the DWH subsurface oil plume documented during the summer of 2010 appears to have been towards the southwest, flowing along a layer of neutral density and paralleling nearshore bathymetric contours of the northern GOM (Parsons and Cross, 2010), in an area unsampled by this survey. This deep trajectory, combined with model results that incorporate oil degradation and dispersion (Adcroft *et al.*, 2010), and evidence for shortened oil particle longevity in the water column as a result of microbial degradation (Hazen *et al.*, 2010; Valentine *et al.*, 2010; Joye *et al.*, 2011) is entirely consistent with the fact that we only observed evidence of a subsurface oil plume in our O_2 and CDOM profiles at a small number of stations within close proximity to the MC252 wellhead.

By August 2010, the zonally-elongated EF had translated southward and once again reattached to the LC (Fig. 1h). However, with no strong circulation north of 27°N, no detectable oil *en route* prior to August, and no additional MC252 oil entering the Gulf following July 15, it is unlikely that any contaminants were available for entrainment into this circulation. However, despite the fact that MC252 oil never reached south Florida beaches, damage to Florida tourism and coastal economies throughout the state [need econ ref here.] did result from the perception~~fear~~ that such an event ~~might have occurred~~was likely.

The fortuitous series of oceanographic events observed during spring/summer 2010 in the GOM, described herein, virtually eliminated the direct pathway from the DWH oil spill site to the coastal environments of south Florida, thus preventing the oil from reaching south Florida waters. It is, however, important to note that this wouldn't necessarily be the case "next time" as there is a well established potential direct pathway from the northern GOM to south Florida when the LC is elongated but the LCR separation process has not yet begun.

6. References

[NOTE - CHRIS AND MICHELLE PLEASE COMPLETE WITH ALL OF YOUR REFERENCES, THEN I WILL PROOFREAD AND FINALIZE - LIBBY]

Adcroft, A., R. Hallberg, J. P. Dunne, B. L. Samuels, J. A. Galt, C. H. Barker, and D. Payton, 2010. Simulations of underwater plumes of dissolved oil in the Gulf of Mexico. Geophys. Res. Lett., 37, pages...

Atwood, ~~1987.~~D. K., F. J. Burton, J. E. Corredor, G. R. Harvey, and A. J. Mata-Jimenez. 1987. Results of the CARIPOL PetroleumPollution Monitoring Project in the Wider Caribbean. Mar. Pollut. Bul. 18:540-48.

Behringer, D. W., R. L. Molinari, and J. F. Festa, 1977. The variability of anticyclonic current patterns in the Gulf of Mexico. J. Geophys. Res., 82(34), 5469-5476.

Brooks, D. A., 1984. Current and hydrographic variability in the northwestern Gulf of Mexico. J. Geophys. Res., 89(C5), 8022-8032.

Brooks, D. A., and R. V. Legeckis, 1982. A ship and satellite view of hydrographic features in the western Gulf of Mexico. J. Geophys. Res., 87(C6), 4195-4206.

Bugden ~~et al., 2008.~~J. B. C. , C. W. Yeung, P. E. Kepkay, and K. Lee. 2008. Application of ultraviolet fluorometry and excitation-emission matrix sprectroscopy (EEMS) to fingerprint oil and chemically dispersed oil seawater. Mar. Pollut. Bul. 56:677-585.

Camilli et al., 2010.

Candela, J., J. Sheinbaum, J. Ochoa, and A. Badan, 2002. The potential vorticity flux through the Yucatan Channel and the Loop Current in the Gulf of Mexico. Geophys. Res. Lett., 29(22), pages...

Cochrane, J. D., 1972. Separation of an anticyclone and subsequent developments in the Loop Current (1969). *Contributions on the Physical Oceanography of the Gulf of Mexico*, L. R. A. Capurro and J. L. Reid, Eds., Gulf Publishing, 91-106.

Diercks ~~et al., 2010~~A-R., R. C. Highsmith, V. L. Asper, D. Joung, Z. Zhou, L. Guo, A. M. Shiller, S. B. Joye, A. P. Teske, N. Guinsso, T. L. Wade, and S. E. Lohrenz. Geophys. Res. Let. 37: page nos??.

Elliot, B. A., 1982. Anticyclonic rings in the Gulf of Mexico. J. Phys. Oceanogr., 12, 1292-1309.

Forristall, G. Z., K. J. Schaudt, and C. K. Cooper, 1992. Evolution and kinematics of a Loop Current eddy in the Gulf of Mexico during 1985. J. Geophys. Res., 97(C2), 2173-2184.

Green, D., B. Humphrey, and B. Fowler. 1983. The use of flow-through fluorometry for tracking dispersed oil. *Proceeding of the 1983 Oil Spill Conference*, pp. 473-478.
~~Green et al., 1983.~~

Hamilton, P., G. S. Fargion, and D. C. Biggs, 1999. Loop Current eddy paths in the western Gulf of Mexico. J. Phys. Oceanogr., 29, 1180-1207.

Hazen, T. C., E. A. Dubinsky, T. Z. DeSantis, G. L.Andersen, Y. M. Piceno, N. Singh, J. K. Jansson, A. Probst, S. E. Borglin, J. L. Fortney, W. T.Stringfellw, M. Bill, M.E. Conrad, L. M. Tom, K. L. Chavarria, T. R. Alusi, R. Lamendella, D. C. Joyner, C. Spier, J. Baelum, M. Auer,

M. L. Zemla, R. Chakraborty, E. L. Sonnenthal, P. D'haseseleer, H-Y. N. Holman, S. Osman, Z. Lu, J. D. Van Nostrand, Y. Deng, J. Zhou, O. U. Mason. 2010. Deep-sea poil plume enriches indigenous oil-degrading bacteria. Science. 330:204-208.

~~et al., 2010.~~

Henry, C.B., P.O. Roberts, E.B. Overton. 1999. A primer on *in situ* fluorometry to monitor dispersed oil. *Proceeding of the 1999 Oil Spill Conference*, pp. 246-250.

~~Henry et al., 1999.~~

Hetland, R. D., Hsueh, Y., Leben, R. R., and P. P. Niiler, 1999. A Loop Current-induced jet along the edge of the west Florida shelf. Geophys. Res. Lett., 26(15), 2239-2242.

Hofmann, E., and S. J. Worley, 1986. An investigation of the circulation of the Gulf of Mexico. J. Geophys. Res., 91(C12), 14,221-14,236.

Hu CM, Muller-Karger FE, Vargo GA, Neely MB, Johns E (2004) Linkages between coastal runoff and the Florida Keys ecosystem: A study of a dark plume event. Geophys Res Lett 31:-

~~Hu et al., 2005.~~

Huh, O. K., W. J. Wiseman, Jr., and L. J. Rouse, Jr., 1981. Intrusion of Loop Current waters onto the west Florida continental shelf. J. Geophys. Res., 86(C5), 4186-4192.

Joyce, P. 1988. Floating tar in the western North Atlantic and Caribbean Sea, 1982-1996. Baseline. 36:167-171.

Joye, S. B., I. R. Macdonald, I. Leifer, and V. Asper. 2011. Magnitude and oxidation potential of hydrocarbon gases released from the BP oil well blowout. Nature Geoscience. Published online 13 February 2011 DOI 10:1038/NGEO1067.
~~et al., 2011.~~

Kessler, J. D., D. L. Valentine, M. C. Redmond, M. Du, E. W. Chan, S. D. Mendes, E. W. Quiroz, C. J. Villanueva, S. S. Shusta, L. M. Werra, S. A. Yvon-Lewis, T. C. Weber. A persistant oxygen anomaly reveals the fate of spilled methane in the deep Gulf of Mexico. Science. 331:312-315.
~~et al., 2011.~~

Leipper, D. F., 1970. A sequence of current patterns in the Gulf of Mexico. J. Geophys. Res., 75(3), 637-657.

Liu, Y., R. H. Weisberg, C. Hu, and L. Zheng, 2011. EOS, Trans. AGU, 92(6), 45-52.

Lumpkin, R. and M. Pazos, 2006: Measuring surface currents with Surface Velocity Program drifters: the instrument, its data, and some recent results. Chapter two of Lagrangian Analysis and Prediction of Coastal and Ocean Dynamics (LAPCOD) ed. A. Griffa, A. D. Kirwan, A. J. Mariano, T. Ozgokmen, and T. Rossby.

Maltrud, M., S. Peacock, and M. Visbeck, 2010. On the possible long-term fate of oil released in the Deepwater Horizon incident, estimated using ensembles of dye release simulations. Env. Res. Lett., 5, pages...

Meinen et al., 2010.

Meyers, S. D., E. M. Siegel, and R. H. Weisberg, 2001. Observations of currents on the west Florida shelf. Geophys. Res. Lett., 28(10), 2037-2040.

Molinari, R. L., J. F. Festa, and D. W. Behringer, 1978. The circulation in the Gulf of Mexico derived from estimated dynamic height fields. J. Phys. Oceanogr., 8, 987-996.

Morey, S. L., P. J. Martin, J. J. O'B., A. A. Wallcraft, and J. Zavala-Hidalgo, 2003. Export pathways for river discharged fresh water in the northern Gulf of Mexico. J. Geophys. Res., 108(C10), pages...

Nowlin, W. D., Jr., 1972. Winter circulation patterns and property distributions. *Contributions on the Physical Oceanography of the Gulf of Mexico*, L. R. A. Capurro and J. L. Reid, Eds., Gulf Publishing, 3-52.

Nowlin, W. D., Jr., and J. M. Hubertz, 1972. Contrasting summer circulation patterns for the eastern Gulf. *Contributions on the Physical Oceanography of the Gulf of Mexico*, L. R. A. Capurro and J. L. Reid, Eds., Gulf Publishing, 3-52.

Nowlin, W. D., Jr., and H. J. McLellan, 1967. A characterization of the Gulf of Mexico waters in winter. J. Mar. Res., 25(1), 29-59.

Oey, L. -Y., T. Ezer, G. Forristall, C. Cooper, S. DiMarco, and S. Fan, 2005. An exercise in forecasting Loop Current and eddy frontal positions in the Gulf of Mexico. Geophys. Res. Lett., 32, pages...

Oey, L. -Y., T. Ezer, and H. -C. Lee, 2005. Loop Current, rings, and related circulation in the Gulf of Mexico: A review of numerical models and future challenges. In: *Circulation in the Gulf of Mexico: Observations and Models*, W. Sturges and A. Lugo-Fernandez, Eds., Geophysical Monograph Ser., American Geophysical Union, Washington, D. C., Vol. 161, 31-56.

Ortner PB, Lee TN, Milne PJ, Zika RG, Clarke ME, Podesta GP, Swart PK, Tester PA, Atkinson LP, Johnson WR (1995) Mississippi River Flood Waters That Reached the Gulf-Stream. Journal of Geophysical Research-Oceans 100:13595-13601
~~Ortner et al., 1995.~~

Paluszkiewicz, T., L. P. Atkinson, E. S. Posmentier, and C. R. McClain, 1983. Observations of a Loop Current frontal eddy intrusion onto the west Florida shelf. J. Geophys. Res., 88(C14), 9639-9651.

Parsons, A. R., and S. L. Cross (2010), A collaborative report on the synthesis of subsurface data from the Deepwater Horizon response effort, Abstract OS21G-04 presented at 2010 Fall Meeting, AGU, San Francisco, Calif., 13-17 Dec.

~~Romero et al., 1981.~~Romero, G. C., G. R. Harvey, and D. K. Atwood. 1981. Stranded tar on Florida beaches: September 1979-October 1980. Mar. Pol. Bul. 12:280-84.

Schroeder, W. W., L. Berner, Jr., and W. D. Nowlin, Jr., 1974. The oceanic waters of the Gulf of Mexico and Yucatan Strait during July 1969. Bull. Mar. Sci., 24 (1), 1-19.

Srinivasan et al., 2010.

Smith et al., 2010.

SMU AGU reference.

Sturges, W., and J. C. Evans, 1983. On the variability of the Loop Current in the Gulf of Mexico. J. Mar. Res., 41, 639-653.

Sturges, W., J. C. Evans, S. Welsh, and W. Holland, 1993. Separation of warm-core rings in the Gulf of Mexico. J. Phys. Oceanogr., 23, 250-268.

Sturges, W., and K. E. Kenyon, 2008. Mean flow in the Gulf of Mexico, J. Phys. Oceanogr., 38, 1501-1514.

Sturges, W., and R. Leben, 2000. Frequency of ring separations from the Loop Current in the Gulf of Mexico: A revised estimate. J. Phys. Oceanogr., 30, 1814-1819.

Valentine, ~~2010.~~D. L. J. D. Kessler, M. C.Redmond, S. D. Mendes, M. B. Heintz, C. Farwell, L. Hu, F. S. Knnaman, S. Yvon-Lewis, M.Du, E. W. Chan, F. G. Tigreros, C. J. Villanueva. Science. 330:208-211.

Van Vleet, E. S., W. M. Sackett, F. F. Weber, and S. B. Reinhardt. Input of pelagic tar into the Northwest Atlantic from the Gulf Loop Current: chemical characterization and its relationships fot weathered IXTOC-I oil. 1983, Can J.Fish. Aquat. Sci. 40(Suppl2):12-22.

Vukovich, F. M., 1995. An updated evaluation of the Loop Current's eddy-shedding frequency. J. Geophys. Res., 100(C5), 8655-8659.

Vukovich, F. M., and B. Crissman, 1986. Aspects of warm core rings in the Gulf of Mexico. J. Geophys. Res., 91(C2), 2645-2660.

Vukovich, F. M., and G. A. Maul, 1985. Cyclonic eddies in the eastern Gulf of Mexico. J. Phys. Oceanogr., 15, 105-117.

Wiseman, W. J., Jr., and S. P. Dinnel, 1988. Shelf currents near the mouth of the Mississippi River. J. Phys. Oceanogr., 18, 1287-1291.

Zavala-Hidalgo, J., S. L. Morey, J. J. O'Briend, and L. Zamudio, 2006. On the Loop Current eddy shedding variability, Atmosfera, 19(1), 41-48.

Table 1. Objective description of θ-S profile grouping criteria [RS IN PROGRESS!].

Table 2. Median and variability of surface water properties [CK].

[-we may not need this table – Ryan]

		Valid N	Median	Range	Std.Dev.
CSW	Salinity	875	35.638	22.406 - 36.517	5.010
	Chl a Flr	875	0.159	0.095 - 4.804	1.086
	CDOM Flr	705	0.090	0.04151 - 0.37668	0.091
GCW	Salinity	2496	36.284	23.742 - 36.49833	3.062
	Chl a Flr	2496	0.097	0.063 - 4.804	0.964
	CDOM Flr	2496	0.076	0.040 - 0.296	0.049
Mixed GCW & LC	Salinity	1449	36.257	31.382 - 36.558	0.821
	Chl a Flr	1449	0.101	0.058 - 0.240	0.036
	CDOM Flr	1380	0.076	0.042 - 0.126	0.014
LCW	Salinity	1243	36.186	35.404 - 36.503	0.125
	Chl a Flr	1243	0.097	0.075 - 0.114	0.008
	CDOM Flr	385	0.077	0.075 - 0.080	0.001
EFCW	Salinity	1143	36.538	36.192 - 36.674	0.072
	Chl a Flr	1143	0.079	0.067 - 0.107	0.008
	CDOM Flr	1143	0.040	0.039 - 0.075	0.013

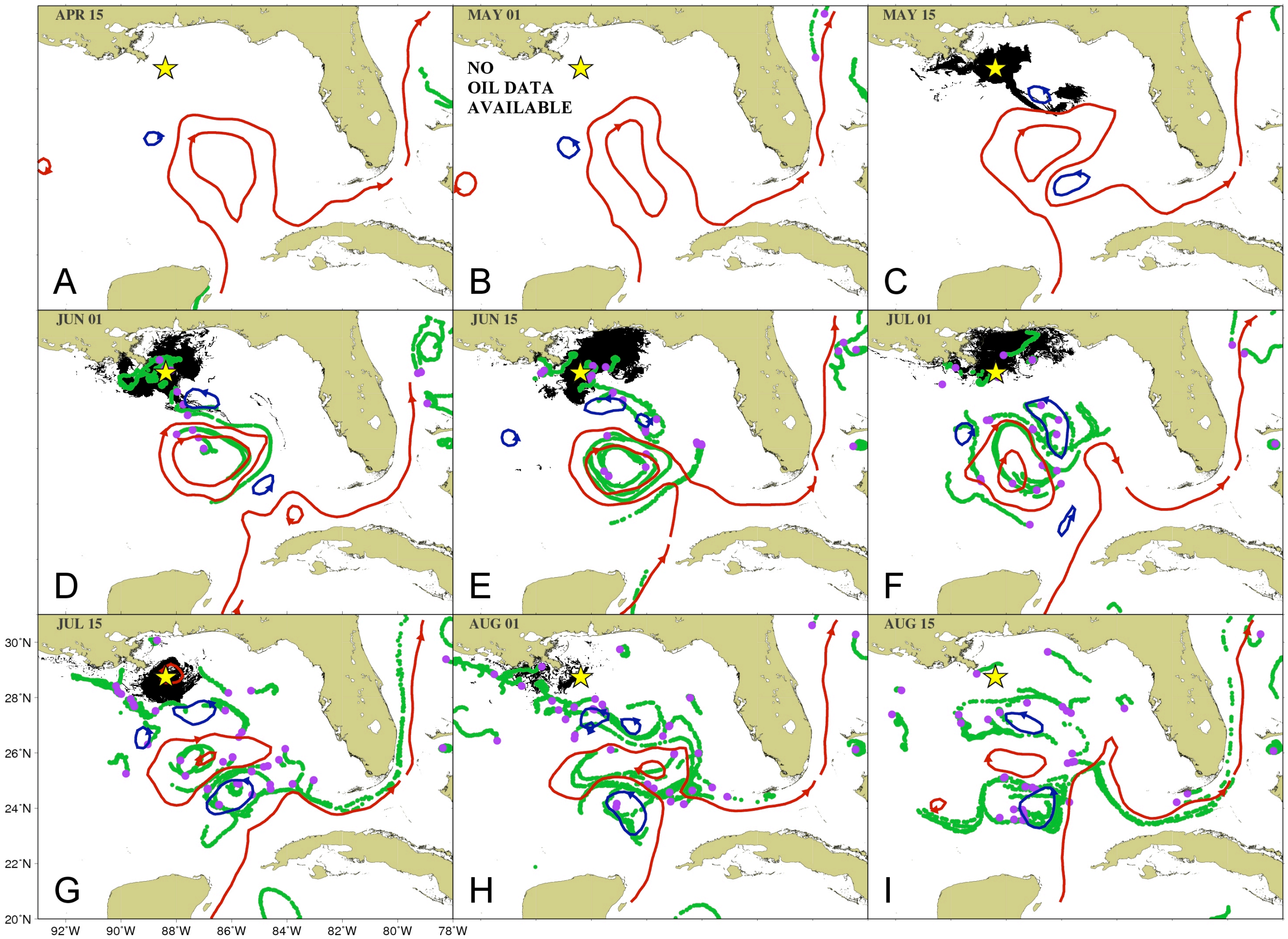

Figure 1. Altimetry-derived surface features, Lagrangian surface drifter trajectories, and the NESDIS/SAB daily surface oil coverage product are shown in the panels above for the GoM from April 15, 2010 through August 15, 2010 (at 15-day intervals). Red lines show the main anti-cyclonic features (LC and EF), and blue lines show indicate cyclonic circulation. 11-day surface drifter trajectories (centered about the date of the plot) are represented as green lines with a purple marker indicating their position at the beginning of the 11-day period. The regions in black denote the extension of the surface oil spill as derived from the daily Experimental Marine Pollution Surveillance Reports produced by NOAA/NESDIS/SAB.

1169 DCP casts.